

magnitude, and it is affected markedly by different dispersion corrections. For example, for the 111 reflection, applying  $f'_{\text{Cu}} = -1.31$  (Matsushita & Kohra, 1974) yields  $F_{\text{VAL}} = -7.62$ , a 19% difference compared with the result in Table 2 obtained with the dispersion correction of Creagh (1988). That part of the observed structure factor which gives information about the non-spherical part of the electron-density distribution is therefore dramatically affected by the magnitude of the dispersion correction.

Within the limitations of the data, it is possible to identify qualitative deformation-density features in the interstitial regions of the crystal which, as previously noted, have no parallels in either silicon or diamond. A better data set is needed to decide whether these features are real or are an artefact of the present limited data (for example, a result of series termination or errors in one or more observations). It is envisaged that a better data set would have the following features.

Firstly, as previously noted by Dawson (1967), accurately scaled data are vital. In the present analysis the two data sets were on different scales which complicated the merging procedure and added one extra variable to the model. Secondly, even greater precision should be aimed for. Thirdly, an accurate experimental determination of the dispersion correction for the appropriate wavelength would remove some doubt from the analysis. Collection of data at a wavelength for which this correction is very small would also lessen this uncertainty. Lastly, a much more extensive data set [out to  $(\sin \theta)/\lambda \geq 1.0 \text{ \AA}^{-1}$

for example] would remove many of the difficulties encountered in the present analysis.

#### References

- BAKER, J. F. C. & HART, M. (1975). *Acta Cryst.* **A31**, 364–367.  
 BALBÁS, L. C., RUBIO, A., ALONSO, J. A., MARCH, N. H. & BORSTEL, G. (1988). *J. Phys. Chem. Solids*, **49**, 1013–1017.  
 BROWN, A. S. & SPACKMAN, M. A. (1989). *Chem. Phys. Lett.* **161**, 427–431.  
 CLEMENTI, E. & RAIMONDI, D. L. (1963). *J. Chem. Phys.* **38**, 2686–2689.  
 CLEMENTI, E. & ROETTI, C. (1974). *At. Data Nucl. Data Tables*, **14**, 177–478.  
 CREAGH, D. C. (1988). *Aust. J. Phys.* **41**, 487–501.  
 CROMER, D. T. (1965). *Acta Cryst.* **18**, 17–23.  
 DAWSON, B. (1967). *Proc. R. Soc. London Ser. A*, **298**, 395–401.  
 DEUTSCH, M. & HART, M. (1985). *Acta Cryst.* **A41**, 48–55.  
 HASTINGS, J. B. & BATTERMAN, B. W. (1975). *Phys. Rev. B*, **12**, 5580–5584.  
 LUDEWIG, J. (1973). *Z. Naturforsch. Teil A*, **28**, 1204–1213.  
 MAIR, S. L. & BARNEA, Z. (1975). *J. Phys. Soc. Jpn*, **38**, 866–869.  
 MATSUSHITA, T. & KOHRA, K. (1974). *Phys. Status Solidi*, **24**, 531–541.  
 ROBERTO, J. B., BATTERMAN, B. W. & KEATING, D. T. (1974). *Phys. Rev. B*, **9**, 2590–2599.  
 SPACKMAN, M. A. (1986). *Acta Cryst.* **A42**, 271–281.  
 SPACKMAN, M. A. & STEWART, R. F. (1984). In *Methods and Applications in Crystallographic Computing*, edited by S. R. HALL & T. ASHIDA, pp. 302–320. Oxford: Clarendon Press.  
 SPACKMAN, M. A. & STEWART, R. F. (1986). Unpublished paper.  
 STEWART, R. F. (1973). *J. Chem. Phys.* **58**, 1668–1676.  
 STEWART, R. F. (1976). *Acta Cryst.* **A32**, 565–574.  
 TAKAMA, T. & SATO, S. (1981). *Jpn. J. Appl. Phys.*, **20**, 1183–1189.  
 WANG, C. S. & KLEIN, B. M. (1981). *Phys. Rev. B*, **24**, 3393–3416.  
 WILLIS, B. T. M. & PRYOR, A. W. (1975). *Thermal Vibrations in Crystallography*. Cambridge Univ. Press.  
 YIN, M. T. & COHEN, M. L. (1982). *Phys. Rev. B*, **26**, 5668–5687.

*Acta Cryst.* (1990). **A46**, 387–393

## On the Quantitative Determination of Triplet Phases by X-ray Three-Beam Diffraction

BY E. WECKERT AND K. HÜMMER

*Institut für Angewandte Physik, Lehrstuhl für Kristallographie der Universität, Bismarckstrasse 10, D-8520 Erlangen, Federal Republic of Germany*

(Received 1 May 1989; accepted 8 December 1989)

### Abstract

Calculations of the integrated diffracted intensity for Renninger experiments, *i.e.* calculations of  $\psi$ -scan profiles scanning through three-beam positions, are reported. The fundamental equations of the dynamical theory are solved by means of an eigenvalue procedure and boundary conditions consistent with the diffraction geometry. It is shown that for non-centrosymmetric structures the three-beam  $\psi$ -scan profiles bear information on both the magnitude, defined in the range  $0 \leq |\phi| \leq 180^\circ$ , and the sign of

the triplet phase involved in the three-beam interference. In general, the  $\psi$ -scan profiles can be separated into two parts: a phase-dependent part ('ideal' profile) due to the interference effect and a symmetric phase-independent *Umweganregung* or *Aufhellung* profile due to the mean energy flow in a three-beam case. Both parts can be calculated by summing up the  $\psi$ -scan profiles for  $+\phi$  and  $-\phi$ , one profile being reversed with respect to the three-beam point. As a result, the experimentally best suited three-beam cases for triplet phase determination should involve structure factors of nearly equal magnitude.

### 1. Introduction

In a recent paper (Hümmer, Weckert & Bondza, 1989) we reported on the direct measurements of triplet phases by means of three-beam interference experiments for two non-centrosymmetric structures. It was shown that the shape of the  $\psi$ -scan intensity profile is related to the triplet phase so that the sign of the triplet phase and not only its cosine can be determined. For example, the  $\psi$ -scan profiles for triplet phases near  $+90$  or  $-90^\circ$  show typical differences. In order to distinguish experimentally between triplet phases of  $+90$  or  $-90^\circ$  it is essential that the structure factors involved in the three-beam case have approximately the same magnitudes. If this criterion is not fulfilled then phase-independent effects of *Aufhellung* or *Umweganregung* superimposed on the interference effect are dominant and it is difficult to extract any phase information.

In order to provide a reliable theoretical basis for the experimental results we resumed our calculations based on Laue's dynamical theory of three-beam X-ray diffraction (*cf.* Hümmer & Billy, 1982). We investigated systematically the influence of the magnitude of the structure factors and we varied systematically the value of the triplet phase to get an idea of the precision of the triplet phases determined from  $\psi$ -scan profiles, when unavoidable phase-independent *Umweganregung* or *Aufhellung* effects are present, as is the case in most three-beam experiments.

Alternative mathematical descriptions of three-beam diffraction related to experimental phase determination are, for example, those of Thorkildsen (1987) who used Takagi-Taupin equations and of Chang & Tang (1988) who used a modified two-beam approximation.

### 2. Computational details

The fundamentals for calculating  $\psi$ -scan profiles near a three-beam case have already been outlined in a former paper (Hümmer & Billy, 1982). Below, this paper is referred to as HBI. In some details we have changed and improved the computing program, to take asymmetric reflection geometries into account.

In the case of asymmetric diffraction geometries the cross sections of the beams depend on the orientations of the normals  $\mathbf{N}$  of the entrance and exit surface with respect to the wave vectors  $\mathbf{K}_n$  of the various beams. In consequence, the reflectivity in the two-beam case must be calculated as (Laue, 1960)

$$R = |\gamma_n| |D_n|^2 / |\gamma_0| |D_0|^2, \quad (1)$$

with

$$\gamma_n = \mathbf{N} \cdot \mathbf{S}_n, \quad \mathbf{S}_n = \mathbf{K}_n / |\mathbf{K}_n|.$$

The  $\gamma$  factors are the direction cosines of the wave vectors with respect to the inward-pointing surface

normal. They are positive or negative for Laue and Bragg cases, respectively.

Therefore, in the three-beam case  $0/h/g$  new amplitudes  $B_n$  of the wavefields are introduced by substitution in equation (8) of HBI (see also Pinsker, 1978) with the expression

$$B_n = \gamma_n^{1/2} D_n. \quad (2)$$

Then, the dynamic fundamental equations for the three-beam case  $0/h/g$  can be written as

$$\begin{aligned} & [-(S_{ym}V_y + S_{zm}V_z)/\gamma_m] B_m^\sigma + [\Gamma/(\gamma_m\gamma_n)^{1/2}] \\ & \times \sum_n F(\mathbf{m}-\mathbf{n})(B_n^\sigma \boldsymbol{\sigma}_m \cdot \boldsymbol{\sigma}_n + B_n^\pi \boldsymbol{\sigma}_m \cdot \boldsymbol{\pi}_n) = V_x B_m^\sigma \\ & [-(S_{ym}V_y + S_{zm}V_z)/\gamma_m] B_m^\pi + [\Gamma/(\gamma_m\gamma_n)^{1/2}] \\ & \times \sum_n F(\mathbf{m}-\mathbf{n})(B_n^\sigma \boldsymbol{\pi}_m \cdot \boldsymbol{\sigma}_n + B_n^\pi \boldsymbol{\pi}_m \cdot \boldsymbol{\pi}_n) = V_x B_m^\pi \end{aligned} \quad (3)$$

with  $\Gamma = r_e \lambda^2 / \pi V_c$  of the order of  $10^{-7}$ – $10^{-8}$ , for  $m$ ,  $n = 0, h, g$ . Here  $r_e$  is the classical electron radius,  $V_c$  the unit-cell volume and  $F(m)$  the structure factor of reflection  $m$ .  $S_{ym}$ ,  $S_{zm}$  refer to a coordinate system where the  $x$  axis is parallel to the surface normal  $N(S_{xm} = \gamma_m)$ , the  $z$  axis lies in the  $K_0$ ,  $K_h$  reflection plane and the  $y$  axis is perpendicular to  $x$  and  $z$ .  $V_y$  and  $V_z$  fix the direction of the incident beam. The diffraction geometry is fixed by the  $\gamma$  factors. The unknown eigenvalues  $V_x$  give the tie points on the dispersion surface.  $B$  are the components of the wavefield amplitudes for  $\pi$  and  $\sigma$  polarization.  $\boldsymbol{\pi}_m$ ,  $\boldsymbol{\sigma}_m$  are unit vectors.  $\boldsymbol{\pi}_m$  is parallel to the  $0-h$  reflection plane,  $\boldsymbol{\sigma}_m$  is perpendicular to  $\boldsymbol{\pi}_m$  and  $\mathbf{S}_m$ .

The solutions of the fundamental equations depend on the diffraction geometry. In a three-beam Laue-Laue case\* the scattering  $S$  matrix is Hermitian. In this case, neglect of anomalous dispersion and a change of sign of the triplet phase  $\phi$  means transposition of the  $S$  matrix. So the eigenvectors are complex conjugates for triplet phases with different signs  $+\phi$  or  $-\phi$  ( $0 \leq |\phi| \leq 180^\circ$  for non-centrosymmetric structures); *i.e.*, in both cases the wave fields belonging to one individual tie point have the same magnitude, but their phases are opposite. If there is any Bragg case involved the  $S$  matrix becomes non-Hermitian.

In calculating the integrated intensity of the primary reflected beam  $I_h(\psi)$  for a  $\psi$ -scan experiment scanning through a three-beam position one encounters difficulties with *Pendellösung* effects in the Laue-Laue and Laue-Bragg diffraction geometries. The intensity oscillates periodically between the beams depending on the thickness of the crystal plate. As a consequence the  $\psi$ -scan profile for a given triplet phase depends on the thickness. Thus, in cases where

\* Laue-Laue means that both reflections of a three-beam diffraction are Laue transmission cases. Bragg-Laue means that the primary reflected beam is a Bragg case but the secondary beam is a Laue case.

the crystal dimensions are anisotropic, it is difficult or impossible to extract phase information from the profile measurements in Laue transmission cases (Thorkildsen, 1987). If one averages over the *Pendellösung* effects (Batterman & Cole, 1964), that is summing up intensities of the waves belonging to different tie points rather than amplitudes, information on the sign of the triplet phase gets lost because of the complex conjugate eigenvectors.

In the Bragg-Bragg and Bragg-Laue geometries these difficulties do not arise. If the primary reflection is a Bragg-reflected beam no *Pendellösung* effects occur for this beam. Therefore, the calculations reported in this paper also refer to these geometries.

The solution of the eigenvalue problem gives the relative amplitudes of the wave fields for each individual tie point. The absolute amplitudes and phases of the excited wave fields for each individual tie point are fixed by the boundary conditions leaving the triplet phase sum invariant. The amplitudes propagating in the  $K_0$  direction must add up to the amplitude of the incident wave field  $D_0$  at the entrance surface.

$$\sum_j c_j B_{j0}^p = |\gamma_0| D_0^p \quad \text{with } p = \pi, \sigma. \quad (4)$$

The  $c_j$  are complex coefficients for all tie points  $j$ .

The sum of the amplitudes for Laue-diffracted waves must be zero at the entrance surface:

$$\sum_j c_j B_{jg}^p = 0. \quad (5)$$

For Bragg-diffracted beams the boundary conditions must be set up at the exit surface:

$$\sum_j c_j B_{jn}^p \exp(2\pi i \mathbf{K}_{jn} \cdot \mathbf{N}t) = 0 \quad n = h, g; \quad (6)$$

$t$  is the thickness of the crystal plate. In general  $\mathbf{K}_{jn}$  is a complex vector. The reflectivity for the primary  $h$  reflection is then given by

$$R_h^p = \left( \left| \sum_j c_j B_{jh}^\pi \right|^2 + \left| \sum_j c_j B_{jh}^\sigma \right|^2 \right) / |\gamma_0| D_0^p{}^2. \quad (7)$$

For unpolarized incident light it is

$$R_h = \frac{1}{2}(R_h^\pi + R_h^\sigma). \quad (8)$$

The integral intensity  $I_h(\psi)$  is calculated as described in detail in HBI. First, the reflectivity  $R_h(\Omega_i, \psi_j)$  is calculated for each pair of  $\Omega_i$  and  $\psi_j$ . Second, the integral intensity of the two-beam profile for each  $\psi_j = \text{constant}$  is calculated by summing  $I_h(\psi_j) = \sum_i R_h(\Omega_i, \psi_j)$ . Third,  $I_h(\psi_j)$  is convoluted with a Gaussian function; its width refers to the divergence, the spectral width of the incident beam and other broadening effects, like mosaicity.

### 3. Results

All the  $\psi$ -scan profiles are calculated for a two-dimensional infinite crystal plate. Its thickness is always 50  $\mu\text{m}$ .

The calculated  $\psi$ -scan profiles are plotted uniformly. The intensity scale gives the relative change of the integrated two-beam intensity. On the  $\psi$  scale,  $\psi = 0$  gives the exact geometrical three-beam position where the endpoints of both reciprocal-lattice vectors lie simultaneously on the Ewald sphere whose radius is given by the mean wave vector inside the crystal

$$|\mathbf{K}_0| = |\mathbf{k}_0| [1 - \frac{1}{2} \Gamma F(\mathbf{0})]$$

with the vacuum wavelength  $\lambda_0 = 1/|\mathbf{k}_0|$ . For  $\psi < 0$  the second reciprocal-lattice vector terminates inside, for  $\psi > 0$  it terminates outside the Ewald sphere (in-out scan).

To demonstrate the influence of the magnitudes of the structure factors, and the influence of the triplet phase, the  $\psi$ -scan profiles refer to fictitious three-beam cases. For each pair in Figs. 1-3 the set of structure-factor moduli remains unchanged. The phases, however, are arbitrarily adjusted so that they add up to the indicated triplet phase, for it is well known that the solutions do not depend on the individual phases but they depend only on the triple phase sum  $\phi$  (Ewald & Héno, 1968). For each three-beam case  $0/h/g$  the triplet phase is given by  $\phi = -\varphi(h) + \varphi(g) + \varphi(h-g)$ , equivalent to  $\phi = \varphi(-h) + \varphi(g) + \varphi(h-g)$  if anomalous dispersion is not taken into account; that means Friedel's law holds:  $F(\pm h) = |F(h)| \exp i\varphi(\pm h)$ . In each figure caption the structure-factor moduli assumed are given in the sequence  $|F(h)|$ ,  $|F(g)|$ ,  $|F(h-g)|$  for the primary, secondary and coupling reflections, respectively. However, to have definite diffraction conditions the lattice parameters and  $F(\mathbf{0})$  of the test substance L-asparagine are used:  $F(\mathbf{0}) = 321$ ,  $a = 5.58$ ,  $b = 9.81$ ,  $c = 11.79$  Å. With this value of  $F(\mathbf{0})$  the chosen crystal thickness of 50  $\mu\text{m}$  is approximately twice the penetration depth of the primary Bragg-reflected beam. All  $\psi$ -scan profiles are calculated with constant diffraction geometry: the reflections  $h = 040$ ,  $g = 042$ , the surface normal  $[0\bar{1}0]$  and the wavelength  $\lambda = 1.54$  Å are used. The integrated profiles are convoluted with a Gaussian profile whose full width at half height is  $5 \times 10^{-30}$ .

The  $\psi$ -scan profiles for  $\phi$  and  $180^\circ - \phi$  are related by a mirror line through  $\psi = 0$ . So the 'in-out'  $\psi$ -scan profile for  $\phi$  is equal to the 'out-in' profile for  $180^\circ - \phi$ . Therefore, examples in the range  $0 \leq |\phi| \leq 90^\circ$  are given here, with one exception in Fig. 1(a).

#### 3.1. Ideal $\psi$ -scan profiles

So-called 'ideal profiles' are plotted in Fig. 1. It can be seen that the increase and decrease of the

two-beam intensity due to constructive and destructive interference effects are of equal size. For example, the two-beam intensities of the 0 or 180° profile are equally enhanced or diminished (Fig. 1a) and the symmetrical increase of the -90° profile is equal to the symmetrical decrease of the +90° profile (Fig. 1b). These profiles can be explained by the interference between the directly (primary) reflected wave and the 'Renninger *Umweg*' wave if this is the dominant process in the three-beam interaction. This is also assumed in the modified two-beam approximation of Hümmer & Billy (1986), where these ideal profiles are derived by a phase-vector diagram. With this construction the typical features of ideal +45 and

-45° profiles can also be derived. The +45° (-45°) profile must have characteristics between those of a 0 and a +90° (-90°) profile. Thus the relative increase of the +45° profile is smaller than the relative decrease and *vice versa* for the -45° profile. This is confirmed by the calculations shown in Fig. 1(c).

This behaviour can be used to give a quantitative definition of an 'ideal profile'. We define a  $\Delta I$  curve by

$$\Delta I(\psi) = \frac{1}{2}[I^+(\psi) + I^-(-\psi)]. \quad (9)$$

$I^+(\psi)$  means the 'in-out'  $\psi$ -scan profile for the positive (+ $\phi$ ),  $I^-(-\psi)$  the 'out-in' profile for the negative (- $\phi$ ) triplet phase. For an ideal  $\psi$ -scan profile  $\Delta I(\psi)$  should remain equal to one. This is valid for the  $\psi$ -scan profiles shown in Fig. 1.

In calculating the  $\psi$ -scan profiles of Figs. 1(a)-(c) the moduli of the structure factors of the primary reflection  $F(h)$ , the secondary  $F(g)$ , and the coupling reflection  $F(h-g)$  given in the figure captions are chosen so that ideal profiles result.

### 3.2. $\psi$ -scan profiles with *Umweganregung* and *Aufhellung*

In discussing these effects we assume for the present that the modulus of the structure factor of the coupling reflection  $F(h-g)$  is approximately equal to that of the primary reflection (but see §3.3). Then, obviously, the  $\psi$ -scan profiles depend on the relative intensities of the primary and secondary reflection. For example, if the *primary* reflection is much weaker than the secondary one, *i.e.* if the primary reflection is (nearly) extinguished (Renninger, 1937), a strong enhancement of the two-beam intensity must result (*Umweganregung*). Then the  $\psi$ -scan profile shows only a very small asymmetry as can be seen from measurements of other authors (Shen & Colella, 1988; Tang & Chang, 1988). On the other hand, if the *secondary* reflection is much weaker than the primary one then a strong reduction in the two-beam intensity must result (*Aufhellung*). Therefore, for the calculations shown in Fig. 2 we change only the ratio  $|F(h)|/|F(g)|$  with respect to the values used in Fig. 1 leaving  $|F(h-g)|$  unchanged.

In Fig. 2 typical *Umweganregung* profiles and in Fig. 3 typical *Aufhellung* profiles are shown for different triplet phases. In each case the  $\Delta I$  curve (9) is plotted.

According to the definition the difference between the  $\psi$ -scan profiles and the corresponding  $\Delta I$  curve leads to ideal profiles. Thus, the profiles with *Umweganregung* and *Aufhellung* can be separated into two parts: (1) the symmetric  $\Delta I$  curve, which is *phase independent* for a specific pair  $\pm\phi$  and which represents the *Umweganregung* or *Aufhellung* effects; and (2) the *phase-dependent* ideal  $\psi$ -scan profiles which are governed by the interference effect bearing the information on the triplet phase.

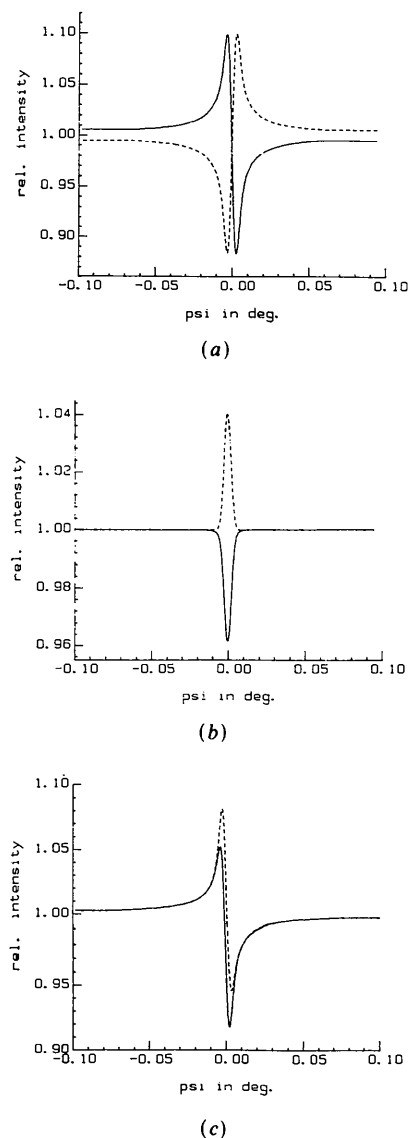


Fig. 1. Ideal  $\psi$ -scan profiles calculated with (a)  $\phi = 0$  (solid) and  $\phi = 180^\circ$  (dashed) and  $|F(m)| = 16, 28, 40$  ( $m = h, g, h-g$ ); (b)  $\phi = +90^\circ$  (solid);  $\phi = -90^\circ$  (dashed);  $|F(m)| = 16, 20, 40$ ; (c)  $\phi = +45^\circ$  (solid);  $\phi = -45^\circ$  (dashed);  $|F(m)| = 16, 24, 40$ .

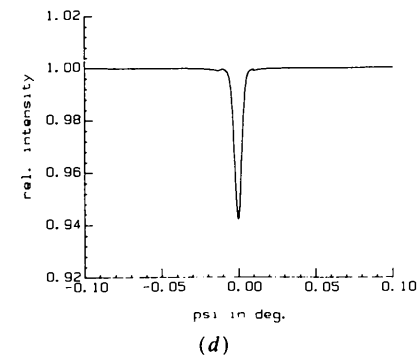
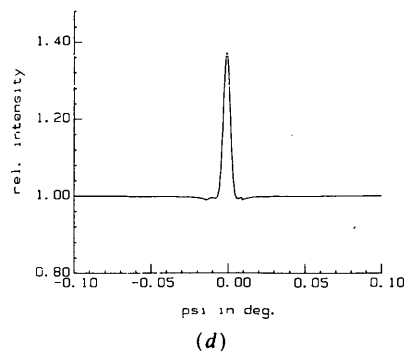
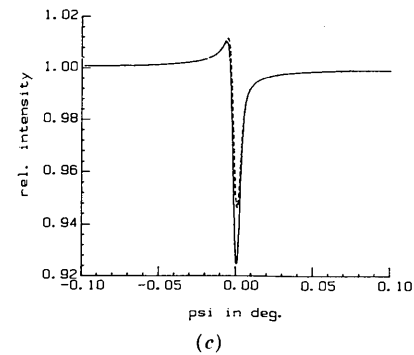
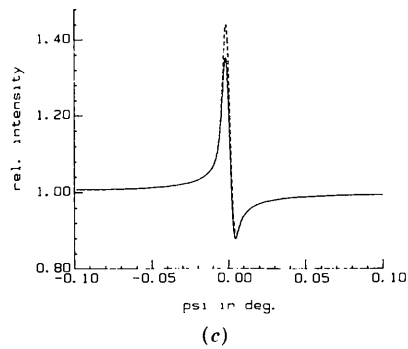
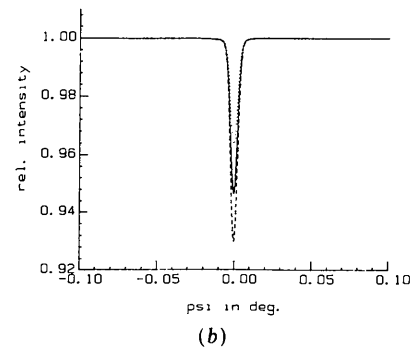
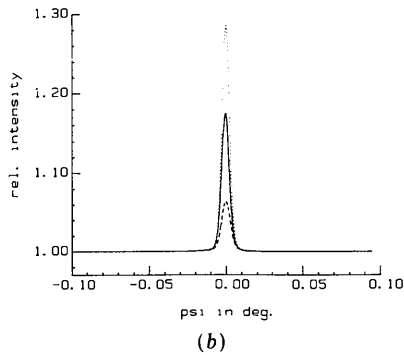
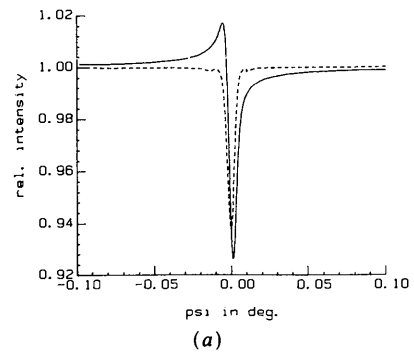
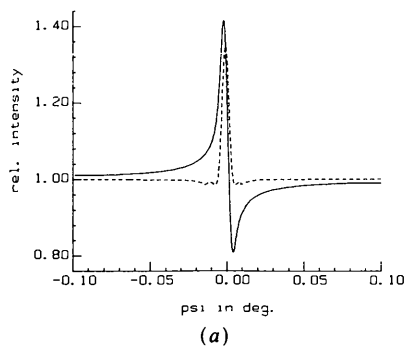


Fig. 2.  $\psi$ -scan profiles with *Umweganregung* and the corresponding  $\Delta I$  curves calculated with: (a)  $\phi = 0^\circ$  (solid);  $\Delta I$  (dashed);  $|F(\mathbf{m})| = 8, 28, 40$ ; (b)  $\phi = +90^\circ$  (dashed);  $\phi = -90^\circ$  (dotted);  $\Delta I$  (solid);  $|F(\mathbf{m})| = 16, 70, 40$ ; (c)  $\phi = +45^\circ$  (solid);  $\phi = -45^\circ$  (dashed);  $|F(\mathbf{m})| = 8, 28, 40$ ; (d)  $\Delta I$  from  $\phi = \pm 45^\circ$ .

Fig. 3.  $\psi$ -scan profiles with *Aufhellung* and the corresponding  $\Delta I$  curves calculated with (a)  $\phi = 0^\circ$  (solid);  $\Delta I$  (dashed);  $|F(\mathbf{m})| = 16, 8, 40$ ; (b)  $\phi = +90^\circ$  (dashed);  $\phi = -90^\circ$  (dotted);  $\Delta I$  (solid);  $|F(\mathbf{m})| = 16, 10, 40$ ; (c)  $\phi = +45^\circ$  (solid);  $\phi = -45^\circ$  (dashed);  $|F(\mathbf{m})| = 16, 8, 40$ ; (d)  $\Delta I$  from  $\phi = \pm 45^\circ$ .

It should be mentioned that with constant structure-factor moduli the magnitudes of the *Umweganregung* and *Aufhellung* depend on the absolute value of the triplet phase. Therefore, in order to obtain ideal  $\psi$ -scan profiles for various triplet phases the structure-factor magnitude of  $F(g)$  was changed (see Fig. 1).

In Figs 2(b) and 3(b) the interference effect of the  $+90^\circ$  profile or of the  $-90^\circ$  profile is overcompensated by *Umweganregung* or *Aufhellung* effects. In spite of this it is possible to extract the triplet phase unambiguously. In Fig. 2(b), for example, as can be seen from the  $\Delta I$  curve the *Umweganregung* is  $+18\%$  and the interference effect is  $-11$  and  $+11\%$  for  $\phi = +90$  and  $\phi = -90^\circ$ , respectively.

If the *Umweganregung* or *Aufhellung* effects are much stronger than the interference effect, then it is difficult to extract reliable phase information from the  $\psi$ -scan profiles, particularly if the triplet phase is not near  $0$  or  $180^\circ$ .

### 3.3. Influence of the coupling reflection

In this section the influence of the magnitude of the structure factor  $F(h-g)$  on the  $\psi$ -scan profile will be discussed. Therefore, the parameters of Fig. 1 remain unchanged except for  $|F(h-g)|$ . If the coupling reflection is weak then the interaction between the diffracted wave fields is weak. Then it is expected that the interference effect is very small and a considerable *Aufhellung* should result because the incident radiation power will be shared between the primary and the secondary reflection. This fact is shown in Fig. 4 for a triplet phase of  $\phi = 0^\circ$  as an example. The solid curve is the  $\psi$ -scan profile calculated with a weak coupling reflection (see figure caption). Calculation of the  $\Delta I$  curve and the ideal  $0^\circ$  profile (not shown in Fig. 4) yields an interference effect of about  $\pm 2\%$ , and an *Aufhellung* effect of nearly  $-5\%$ .

If the structure factor of the coupling reflection is increased the amplitude of the *Umweg* wave is enhanced and, with that, also the interference effect. This is shown in Fig. 4 by the dashed profile. The

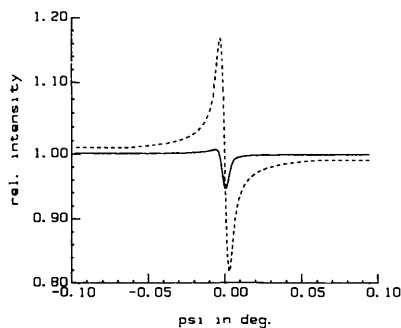


Fig. 4.  $\psi$ -scan profiles for  $\phi = 0^\circ$  with different structure-factor magnitude of the coupling reflection  $|F(\mathbf{m})| = 16, 28, 5$  (solid);  $|F(\mathbf{m})| = 16, 28, 70$  (dashed).

result is an ideal  $0^\circ$  profile; the interference effect is nearly  $\pm 20\%$ .

The secondary ( $g$ ) and coupling ( $h-g$ ) reflections are symmetric with respect to their influence on the primary diffracted intensity. To make things clearer, we discuss their influence separately.

## 4. Discussion

The calculated  $\psi$ -scan profiles give evidence that in general the interference effect, which leads to the so-called ideal profiles, is overlaid by *Umweganregung* and *Aufhellung* effects. The latter are independent of the sign of the triplet phase as they can be evaluated from the  $\Delta I$  curve.

These effects are self-consistently inherent in the dynamic theory. The fundamental equations describe the interference between the excited wave fields (Laue, 1960). As a consequence, the mean energy flow is modulated by the interference according to the phase differences. For example, the intensity resulting from the interference of two waves with amplitudes  $A_1$  and  $A_2$  and phase difference  $\alpha - \beta$  is given by

$$I = |A_1 \exp i\alpha + A_2 \exp i\beta|^2 \\ = A_1^2 + A_2^2 + 2A_1A_2 \cos(\alpha - \beta).$$

$A_1^2 + A_2^2$  gives the mean energy flow, the third interference term gives the modulation.

In a three-beam case the mean energy flow of the  $h$  reflection and  $g$  reflection is governed by the structure-factor moduli  $|F(n)|$ ,  $n = 0, h, g, h-g$ , as the incident power is shared between the two reflections, and these are coupled by  $F(h-g)$ . The mean energy flow due to these mutual interactions can be described by differential equations which have the conservation of energy as a fundamental hypothesis (Moon & Shull, 1964). As a consequence, the interaction terms are taken to be phase independent. If in a three-beam case these couplings are well balanced, then no change of the two-beam intensity would result, except for that due to the interference effects. Thus, this situation leads to ideal profiles.

The calculations based on the dynamic theory clearly demonstrate that *Umweganregung* and *Aufhellung* are multiple scattering effects. However, Chang & Tang (1988) in a recent paper denoted the *Umweganregung* as 'kinematical diffraction intensity'. This is an unfortunate notation, as the kinematic interaction neglects any multiple scattering effects.

The calculations show that the asymmetry of the three-beam  $\psi$ -scan profiles decreases with decreasing  $\cos \phi$ . This fact has been already pointed out by other authors (Juretschke, 1982; Shen & Colella, 1988).

In this work it is repeatedly confirmed that the  $\psi$ -scan profiles depend on the sign of the triplet phase ( $\pm \phi$ ) and not on  $\cos \phi$ . This statement holds without

taking into account anomalous dispersion. This point is extremely important for the experimental determination of the absolute structure (configuration) for light-atom structures.

For the relation between the asymmetry of  $\psi$ -scan profiles and the triplet phase to remain unambiguous some restrictions apply. The foregoing results are true if the relevant scalar products [*cf.* (3)] between the  $\pi$ - and  $\sigma$ -polarization modes are positive. If this is not the case an additional reversal of asymmetry may occur (Juretschke, 1984). These conditions must therefore be checked in order to avoid misinterpretations with respect to the triplet phase.

From the results and discussion it might be speculated that triplet phases can be determined experimentally with relatively high precision, for example, by fitting the experimental and theoretical  $\psi$ -scan profiles. However, experimentally the theoretical assumptions must then be fulfilled: ideal perfect crystal with well oriented perfect faces, definite diffraction geometry, accurately known structure-factor moduli *etc.* With specimens commonly used for X-ray crystal structure determination these requirements can hardly be fulfilled. For the measurements we use crystals with typical dimension from 0.1 to 0.5 mm and grown faces. They are bathed in the incident beam. Thus the incident radiation strikes several faces and a mixture of primary Bragg and Laue cases occurs. In spite of these adversities triplet phases can be measured with a precision of at least 45°, as will be shown in the following paper (Hümmer, Weckert & Bondza, 1990).

Experimentally the *Umweganregung* and *Aufhellung* can be evaluated by comparing  $\psi$ -scan profiles of centrosymmetrically related three-beam cases  $0/h/g$  and  $0/-h/-g$  which have triplet phases with opposite signs but constant structure-factor moduli if anomalous dispersion can be neglected. For precise phase determination however, the *Umweganregung*

or *Aufhellung* effects must be as small as possible. As can be seen from our calculations, ideal profiles result if  $|F(g)|$  and  $|F(h-g)|$  are about twice as strong as  $|F(h)|$ .

These results were reported at the 11th European Crystallographic Meeting in Vienna (Weckert & Hümmer, 1988) and in part at the Fourteenth International Congress of Crystallography in Perth (Hümmer, Bondza & Weckert, 1987; Weckert, Bondza & Hümmer, 1987).

This work has been funded by the Deutsche Forschungsgemeinschaft and the German Federal Minister of Research and Technology under contract No. 05 363 IAI 4.

#### References

- BATTERMAN, B. W. & COLE, H. (1964). *Rev. Mod. Phys.* **36**, 681-717.  
 CHANG, S. L. & TANG, M. T. (1988). *Acta Cryst.* **A44**, 1065-1072.  
 EWALD, P. P. & HÉNO, Y. (1968). *Acta Cryst.* **A24**, 5-15.  
 HÜMMER, K. & BILLY, H. (1982). *Acta Cryst.* **A38**, 841-848.  
 HÜMMER, K. & BILLY, H. (1986). *Acta Cryst.* **A42**, 127-133.  
 HÜMMER, K., BONDZA, H. & WECKERT, E. (1987). *Acta Cryst.* **A43**, C222.  
 HÜMMER, K., WECKERT, E. & BONDZA, H. (1989). *Acta Cryst.* **A45**, 182-187.  
 HÜMMER, K., WECKERT, E. & BONDZA, H. (1990). *Acta Cryst.* **A46**, 393-402.  
 JURETSCHKE, H. J. (1982). *Phys. Lett.* **92A**, 183-185.  
 JURETSCHKE, H. J. (1984). *Acta Cryst.* **A40**, 379-389.  
 LAUE, M. VON (1960). *Röntgenstrahl-Interferenzen*, 3rd ed., p. 343. Frankfurt am Main: Akademische Verlagsgesellschaft.  
 MOON, R. M. & SHULL, C. G. (1964). *Acta Cryst.* **17**, 805-812.  
 PINSKER, Z. G. (1978). *Dynamical Scattering of X-rays in Crystals: Solid State Sciences 3*, edited by M. CARDONA, P. FULDE & H. J. QUEISER, pp. 433 ff. Berlin: Springer.  
 RENNINGER, M. (1937). *Z. Kristallogr.* **97**, 107.  
 SHEN, Q. & COLELLA, R. (1988). *Acta Cryst.* **A44**, 17-21.  
 TANG, M. T. & CHANG, S. L. (1988). *Acta Cryst.* **A44**, 1073-1078.  
 THORKILDSEN, G. (1987). *Acta Cryst.* **A43**, 361-369.  
 WECKERT, E., BONDZA, H. & HÜMMER, K. (1987). *Acta Cryst.* **A43**, C264.  
 WECKERT, E. & HÜMMER, K. (1988). *Z. Kristallogr.* **185**, 454.

*Acta Cryst.* (1990). **A46**, 393-402

## Direct Measurements of Triplet Phase Relationships of Organic Non-Centrosymmetric Structures using Synchrotron Radiation

BY K. HÜMMER, E. WECKERT AND H. BONDZA

*Institut für Angewandte Physik, Lehrstuhl für Kristallographie der Universität, Bismarckstrasse 10, D-8520 Erlangen, Federal Republic of Germany*

(Received 1 May 1989; accepted 8 December 1989)

#### Abstract

Recent progress in experimental triplet phase determination by the method of three-beam diffraction for

non-centrosymmetric light-atom structures is reported. The measurements were carried out with a special  $\psi$ -circle diffractometer installed at the DORIS II storage ring in Hamburg. Experimental results